Progress in Additive Manufacturing (2024) 9:169–183
https://doi.org/10.1007/s40964-023-00441-8

FULL RESEARCH ARTICLE

A novel lightweight mechanism for 3D printing of cementitious materials

Mehrab Nodehi[1] · Liam Omer[1] · Bahram Asiabanpour[1] · Togay Ozbakkaloglu[1]

Received: 24 August 2022 / Accepted: 27 March 2023 / Published online: 24 April 2023

Abstract
Applications of additive manufacturing (AM) in the construction industry started 3 decades ago with the first patent and prototype of the contour crafting process. Since then, its obvious benefits in reducing labor cost and construction waste, while improving efficiency and flexibility, have led to the development of several large-scale commercial machines in this field. However, proper lab-scale machines for training experts in automated construction and research-based activities, such as material optimizations for civil and structural engineers are often costly and require large spaces. The only available small-scale apparatus in AM-based construction is usually limited to being able to print only a minimal list of materials with fine sizes. As a result, those machines are not capable of fabricating samples from cementitious materials with a variety of aggregate sizes. This paper compares two low-cost, modular AM-based construction systems capable of extruding a wide variety of cementitious materials with diverse aggregate sizes. The systems are capable of controlled extrusion with a variety of cross-section forms. Additionally, the systems can be attached to a robotic arm, or other computer numerical control (CNC) machines. As a proof-of-concept, the developed system is utilized to fabricate cement mortar with larger aggregate sizes with varied material compositions. Mechanical performance and shrinkage of the resulting additively manufactured cementitious parts are examined and compared.

Keywords Additive manufacturing · 3D printing cementitious materials · 3D concrete printing · 3D-printed geopolymer

1 Introduction

Since the conceptual development of the fourth industrial revolution (Industry 4.0), additive manufacturing (also 3D printing) has become a vital technology in multiple engineering sectors to align with automation and smartification [1, 2]. The integration of 3D printing with Industry 4.0 has revolutionized the way that products are designed, developed, and manufactured. 3D printing allows for the creation of complex shapes and structures that would often be difficult or even costly to produce using traditional manufacturing techniques [3]. Despite the considerable variation in 3D printers' technologies, it has been proven many times that it can significantly improve efficiency, reduce costs of manufacturing, and increase customization and flexibility in manufacturing processes. In this sense, 3D printers would play a key role in the ongoing transformation of industry brought about by the fourth industrial revolution [4–7]. In general, 3D printers can be categorized based on their method of printing or technologies used. Of the various forms, one can name, fused deposition modeling (FDM), stereolithography (SLA), selective laser sintering (SLS), digital light processing (DLP), binder jetting, material jetting, direct energy deposition, and material extrusion [4, 8].

Starting from the introduction of extrusion-based 3D printing in construction by Khoshnevis [9], major attempts have been made to further enhance and discover the unfolded potentials of this newly born technology (see Fig. 1). Through recent trials, this technology has shown potential to reduce labor costs, and construction waste up to 50 and 30%, respectively [10–12]. However, the lack of formworks

✉ Togay Ozbakkaloglu
Togay.oz@txstate.edu

Mehrab Nodehi
M_N224@txstate.edu

Liam Omer
lmo61@txstate.edu

Bahram Asiabanpour
ba13@txstate.edu

[1] Ingram School of Engineering, Texas State University, San Marcos, TX 78666, USA

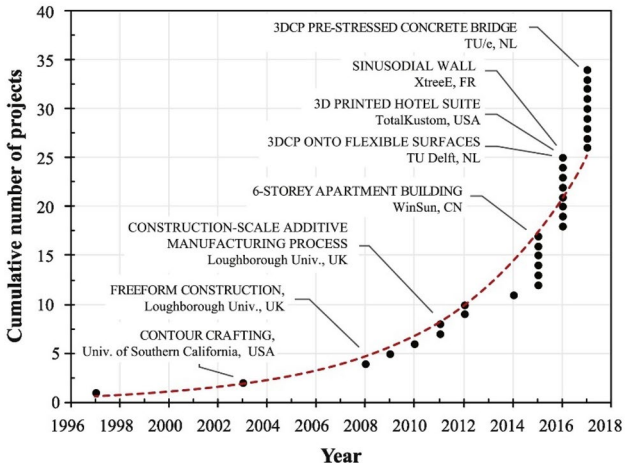

Fig. 1 The progress of 3D concrete printing from the late 1990s–2018 [14]

when 3D printing concrete, has significantly increased the complexity in comparison to current industry processing. Despite this, it is reported that the printed materials most often have a better mechanical properties and geometrical precision [13]. The extrusion of cementitious materials is directly influenced by the fresh properties of the mortar or concrete [14]. Accordingly, rheological properties are the most sensitive properties that can limit the quality of the printed materials. The degree to which rheology contributes to the printing process is in harmony with the printers' designed extruders and nozzles. In other words, the mixture's design should be aligned with the extruder and nozzle's size to be able to effectively print concrete or cementitious materials. On this basis, one of the major issues associated with 3D concrete printing is the materials' roughness and the size. Aggregates that affect the overall viscosity of the extrusion process define the potential extrudability, as well as pumpability of the mixture [15]. In addition, viscosity changes are directly influenced by the content of the binding agents (e.g., cement and supplementary cementitious materials), as well as the size, content, and particle distribution of aggregates.

According to Ref. [14], a binding mixture with plastic viscosity equal to (38.7 ± 4.5) Pa.s (for CEM I & coal fly ash), and (21.1 ± 2.4) Pa.s (for CEM I & limestone filler), are suitable for pumping and extrusion. However, based on the result of Refs. [12, 16–21], the aggregate size must be between one fifth (1/5) to one-tenth (1/10) of the actual nozzle orifice (see Table 1), for the materials to be printable. This is due to the higher yield stress of finer particles [15] and the ability of the printer to pump the materials from a smaller orifice without nozzle obstruction. To reduce the possibility of blockage multiple strategies have been adopted within the literature including:

Table 1 Max aggregate size versus that of nozzle dimensions with successful printing

Reference	Size of aggregate	Nozzle size	Layer height	Sand:binder ratio	Max nozzle diameter to agg size ratio
Moelich et al. (2020) [16]	4.75 mm	25 mm (Circular)	10 mm	1.4	5.2
Ding et al. (2020) [17]	0.9 mm	30 mm (Circle)	15 mm	1	33
Wolfs et al. 2019) [22]	1 mm	N/A	8,9.5,11 mm	N/A	N/A
Sanjayan et al. (2018) [12]	500 µm	25 mm × 15 mm	N/A	1.5	30
Tay et al. (2019) [23]	N/A	30 mm × 15 mm	15 mm	1.2	N/A
Zhang et al. (2019) [15]	1.18, 2.36, 4.75	N/A	N/A	N/A	N/A
Federowicz et al. (2020) [24]	2 mm	20 mm (Circular)	15 mm	1.5	10
Ding et al. (2020) [25]	1.2 mm	30 mm × 15 mm	15 mm	1	12.5
Panda et al. (2019) [18]	2 mm	20 × 20 mm	15 mm	1.22	10
Wang et al. (2020) [26]	0.25 mm	N/A	N/A	N/A	N/A
Ju et al. (2017) [27]	10 mm	N/A	N/A	1.25	N/A
Le et al. (2011) [28]	2 mm	9 mm	N/A	1.5	4.5
Lim et al. (2018) [19]	1.18 mm	13 mm × 30 mm	13 mm	1.5	11
Zhang et al. (2018) [20]	1 mm	20 mm (Circular)	12–15 mm	0.6, 0.8, 1, 1.2, 1.5	20
Pham et al. (2020) [29]	N/A	N/A	6 mm	1	N/A
Panda et al. (2017) [30]	1.15 mm	30 × 15,20 × 20 mm	N/A	N/A	13
Cicione et al. (2020) [31]	4.75 mm	25 mm (Circular)	15 mm	N/A	5.2
Joh et al. (2020) [32]	0.2 mm	N/A	N/A	N/A	N/A
Ting et al. (2019) [33]	N/A	30 × 15 mm	15 mm	1.2	N/A
Chen et al. (2020) [21]	2 mm	40 × 13.5 mm	25–27 mm	1.875	6.75

- *Higher contents of cementitious materials* are used due to increase lubrication and higher geometric stability of materials to sustain their shape while supporting the weight of additional layers.
- *Finer aggregate particles (< 4.75 mm)* are utilized since the mixture with higher yield stress supports buildability [15].
- *Higher use of admixtures* such as high range water reducers, and retarders to elongate the setting time and allow an elongated duration for printing to be performed.
- *Larger orifice nozzles* allows for the extrusion of high aggregate size (> 4.75 mm) and lower force required for successful extrusion.

Due to the initial costs and complexity of multi-systematic operation of the commonly commercialized (extrusion-based) 3D printers, research and development practices require a larger sum of funding for entertaining this novel technology. As a result, in this study, we provide a proof-of-concept on utilizing a simple, functional instrument that can meet the expectations of Civil and Structural engineers by providing a simple means for research and development studies. Unlike most cementitious-material 3D printers that rely on hydraulic pumps, robotic arms, or air pressures, the system of study is based on a simplistic screw-based extrusion using gravity-fed material delivery to reduce the need for the additional systems while providing the ability to 3D print cement mortar with larger aggregate sizes. In the process of optimizing our system, additional extrusion mechanisms and nozzle patterns were designed, fabricated, and tested to determine optimal parameters for the printing of cementitious material regularly used within automated construction applications. In this regard, different mechanisms for pushing cementitious materials and different nozzle patterns were designed, fabricated, and tested so in integration with the optimization efforts on the cement mixture specs they achieve optimum form for the automated construction applications. Depending on the materials viscosity, a gravity-based material feed system, or more advanced pressurized delivery systems, can be coupled with this extrusion system obviating the need for costly instruments that are commonly commercialized. In accordance, a proof-of concept with different materials compositions is provided and their respective mechanical properties are discussed.

2 Components of 3D printing of cementitious materials

Additive manufacturing of concrete consists of an automated robotic arm, a concrete pump, and a print-head (or nozzle). Multiple research platforms such as in Refs. [11, 34, 35], exhibit a specifically dedicated extrusion screw that operates as a material flow controller. Each component can be individually improved rather than purchasing a complete machine reducing the cost of upgrading current machinery. One specific extrusion-based 3D printer, mainly utilized for printing cementitious materials, the Lutum developed by Vormvrij [36] has scaled the various components for small-scale use. The following components are the key ingredients of any 3D printing system for cementitious materials:

- *Pump* A pump transfers mixed material to the nozzle for extrusion. The material rheology is an integral factor in pump requirements as the high viscosity of concrete significantly increases the necessary power for sufficient material delivery. It is also possible for the system to utilize gravity or pre-fed container without using a pump, which is not commonly practiced.
- *Extrusion Screw* An electronically driven extrusion screw provides improved flow control of the high viscosity concrete materials. Material flow from the extruder system is dependent upon the rotation of the auger, its size and speed of operation. The size of extrusion screw and pitch are the limiting factor in usable aggregate size used within a mixture.
- *Robotic arm* An automated and programmed robotic arm, or a gantry system controls the location and position of the extruder system and the nozzle. As a result, the robotic arm is one of the main components of the overall accuracy of the system. Its range of motion defines the size of samples that can be produced.
- *Nozzle* For the deposited materials to have the proper shape and physico-mechanical properties, at the end of the system a designed nozzle shapes the flowing materials to their deposition location. Most commonly, in 3D printing cementitious materials a circular or rectangular nozzle are utilized. With each type having certain benefits, the rectangular nozzle is reported to reduce air-voids between the layer that is commonly observed in previous studies [35]. Additionally, rectangular nozzles are favored in studies that focus on mechanical testing as a result of sections being more comparable to casted materials exhibiting reduced deformation. However, rectangular nozzles also require more complex control systems as they have to contour to the printing path to maintain the rectangular deposition parallel to the desired path.

3 Materials and mixture proportions

3.1 Portland cement

In this study, ordinary Portland cement (CEM type I/II) conforming to ASTM C150, with a CaO content of ~ 64%,

Table 2 Chemical composition of the Portland cement used in this study

Physico-chemical properties of CEM I	
SiO_2 (%)	20.8
Al_2O_3 (%)	5.20
Fe_2O_3 (%)	3.80
CaO (%)	64.3
MgO (%)	1.20
SO_3 (%)	2.0
Na_2O (%)	0.1
K_2O (%)	0.4
LOI (%)	1.3

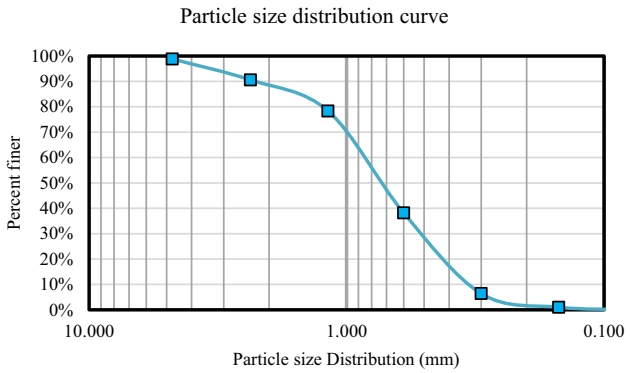

Fig. 2 Particle size distribution of river sand used

Table 3 Showing the result of ASTM C128 [38], conducted on the river sand as part of this study

River sand			
Bulk S.G	Bulk S.G. SSD	Apparent S.G	Absorption (%)
2.61	2.66	2.75	1.93

has been used. Table 2 provides further information on the composition of the Portland cement used in this study.

3.2 Aggregate

River sand with an overall particle size distribution (max < 4.75 mm) illustrated in Fig. 2, was used conforming to ASTM C136 [37]. In addition, Table 3 outlines the bulk, apparent specific gravity, and total absorption of river sand particles, which was tested for this study based on ASTM C128 [38].

3.3 Coal fly ash and GGBFS

Class F coal fly ash and Ground granulated blast-furnace slag (GGBFS) used in this study was supplied by Diversified Minerals (MDI) Inc. from Oxnard, California, with a specific gravity of 2.3–2.7 and 2.93, respectively. Table 4 presents the physico-chemical properties of coal fly ash used in this study.

Table 4 Physico-chemical properties of the coal fly ash (class F) and GGBFS used in this study

Information	Coal fly ash (F)	Blast furnace slag (GGBFS)
SiO_2 (%)	59.12	34.2
Al_2O_3 (%)	20.79	13.68
Fe_2O_3 (%)	5.66	0.75
CaO (%)	7.26	41.41
Na_2O (%)	1.34	–
K_2O (%)	1.27	–
SO_3	0.82	–
MgO	–	6.24
LOI (%)	–	–
Specific gravity	2.3 – 2.7	2.93
Moisture content (%)	0.09	-

3.4 Mixture proportions

In this study, a total of 33 mixes (with one factor difference at a time) have been tested with the instruments to evaluate their potential printability and the quality of the printed materials. Out of the 33 mixes, one mix, shown in Table 5 was chosen to compare the mechanical properties of printed materials using different extrusion mechanisms. The reason for choosing this mix was the authors experience in this research, finding the mentioned mix due to better quality results using different instruments. Figure 3 shows the sieved sands used in this research.

4 Instruments and printing tests

Currently, there are a variety of delivery systems for use within additively manufactured concrete systems. For the scope of this research within concrete extrusion, only fused filament forming additive manufacturing processes will be discussed. Generally, concrete extrusion systems are reliant on material mixing, material delivery, and material deposition. Material mixing ensures appropriate dispersion of constituent materials in addition to appropriate hydration. This is often accomplished through mechanical mixing of the materials in paddle or screw mixers that introduce wall shearing and turbulence within the material to disperse aggregates and additives. Material delivery is usually accomplished through gravity-fed or pump-assisted systems [39]. Gravity-fed systems essentially

Table 5 Mixture proportions adopted as the most suitable for all instruments

Materials	OPC	RS	Water	Fly ash	GGBFS	SP and RT (g)
Proportion	1	0.5	0.33	0.5	0.5	1.3

With SP: superplasticizer and RT: retarder (used in combined form throughout the study)

(a) (b)

Fig. 3 Images of the sieved sands with **a** max size of 4.75 mm and **b** max size of 0.6 mm

create pumping pressure through potential energy provided by the height of the material reservoir being above the deposition head. This method results in higher reliance of the printing system to the viscosity of the materials than the actual gravity energy [40, 41]. Nonetheless, gravity-fed systems provide a simple and cost-effective method for delivering cementitious materials that only requires energy to raise the reservoir to appropriate heights. A pump-assisted system use hydraulic rams to mechanically press materials through either piping or high-pressure hoses to the deposition head, as in Refs. [35, 42]. The advantages to pumping systems are volumetric flow control and material reservoirs at ground level. However, pump systems are inherently expensive due to their hydraulic force systems that include precision rams, motors, manifolds, and high-pressure hoses. In addition, these systems are intended for construction applications that require large volumes of concrete at a given time. The large volume systems are not conducive to small batch experimentation with exploratory additives such as geopolymers and would produce significantly larger amounts of waste than gravity filled canisters. With cost effectiveness and ease of use in mind, a gravity-fed canister was used to deliver material to the screw-based extrusion mechanism presented in this paper. It provides material delivery without the need for power while also providing an opportunity to continuously fill the reservoir during additive manufacturing of large-scale parts.

4.1 Sample sizes and preparations of methodology

Due to the recent inception of concrete based AM, common construction standards and national codes still have not fully regulated specific testing procedures dedicated to 3D printing properties. However, due to additive manufacturing's combined use of spray and self-compacting concrete, most studies tend to conform to the commonly used practices in fresh and hardened state properties of the mentioned materials. In the following subsections, a few of such tests are discussed.

4.2 Fresh properties

In terms of fresh properties, rheological properties, in combination with the commonly used tests conducted for self-compacting concrete, are used. These tests include flow table, mini-slump, v-funnel, torque meter, viscometer and rheometer [43]. In this research study, a flow table is used to measure the flowability of freshly mixed mortar.

4.3 Compressive strength

Conforming to ASTM C109 [44], compressive strength of cube sections are generally cut from a larger material samples and are used to ensure the homogeneity of the printed section when tested [45]. Yet, in some instances such as in Ref. [46] the section is printed to the shape of a cube to

conform the codes available for conventionally cast concrete (e.g., ASTM C109 [44] or C39 [47]). Similar to Ref. [45], in this research, cubic samples are cut from the printed samples to conform to ASTM C109 [44].

4.4 Sample curing

In this study, after the specimens were printed, they were placed in a curing room with an ambient temperature of 23˚C, with a relative humidity of 50%, conforming to ASTM C109 [44] until tested. This value has been selected as it is the most commonly used curing temperature and relative humidity value for curing of the cementitious materials.

4.5 3D printing instruments

4.5.1 Lutum V4

The Lutum V4 is an all-in-one, extrusion-based instrument that is designed for the additive manufacture of clay-based materials. As a part of this study, to provide further insight on the extrudability of different mixes and materials for further comparison, 18 mixes were designed and attempted (one factor at a time). Mixture ratios and their potential printing success is documented in Table 6. Due to the small auger orifice, the system was unable to print cementitious materials with large aggregate sizes common in state-of-the-art concretes. Although this system provides the ability to print controlled geometries using an auger-based delivery system, its cost and small orifice limit its use in experimental concrete construction or experimentation. Figure 4 (a)-(c) provide images of the printer, nozzle orifice and its originally designed extruder.

4.5.2 Piston-based extrusion

Another instrument used to additively manufacture (3D printing) cementitious materials is a piston-based extrusion mechanism, supplied from locally available markets. Figure 5a, b shows the instrument and Fig. 5c shows the nozzles to be used for all tested extrusion instruments presented. Having major similarities to the adhesive containers used in Ref. [48], it can keep cementitious materials within and based on the nozzle of choice, extrude the material through the mechanical force of the rearward piston. The design illustrated below used an additively manufactured thermoplastic die that can be interchanged with other dies to obtain a variety of different nozzle sizes and shapes. The device provides an affordable method for producing extruded concretes samples for testing in

Table 6 Trials conducted with different mixes and different nozzle sizes

Mix no.	Cementitious materials	Sand	Water/Sodium hydroxide	Additive	Max aggregate size	Nozzle size	Printability
1	OPC: 1	–	W: 0.30	–	-	1 mm	No
2	OPC: 1	RS: 1	W: 0.30	–	600 µm	1 mm	No
3	OPC: 1	–	W: 0.33	–	-	7 mm	Yes
4	OPC: 1	RS: 1	W: 0.34	–	600 µm	7 mm	Yes
5	OPC: 1	RS: 1	W: 0.33	–	2 mm	7 mm	Partially
6	OPC: 1	RS: 0.5	W: 0.35	–	2 mm	7 mm	Yes
7	OPC: 1	RS: 1	W: 0.35	–	4.75 mm	7 mm	No
8	OPC: 1	RS: 1	W: 0.35	–	2 mm	10 mm	Yes
9	OPC: 1	RS: 1	W: 0.31	–	2 mm	7 mm	No
10	0.5 OPC – 0.5 FA (C)	RS: 1	SH: 0.8	–	4.75 mm	7 mm	No
11	0.5 OPC – 0.5 FA (C)	RS: 1	SH: 0.8	–	2 mm	10 mm	Partially
12	0.5 OPC – 0.25 FA (C) – 0.25 GGBFS	RS: 1	SH: 0.8	–	+4.75 mm	20×10 mm (90˚)	No
13	0.5 OPC – 0.5 GGBFS	RS: 1	SH: 0.8	–	2 mm	20×10 mm (90˚)	No
14	OPC: 1	RS: 1	W: 0.35	SP 0.007 RET: 0.012	2 mm	20×10 mm (90˚)	No
15	OPC: 1	RS: 1	W: 0.30	SP 0.007 RET: 0.012	2 mm	20×10 mm (90˚)	No
16	OPC: 1	RS: 1	W: 0.30	RET: 0.012	2 mm	20×10 mm (90˚)	No
17	OPC: 1	RS: 1	W: 0.30	–	1 mm	20 mm round	No
18	OPC 2	RS: 1	W: 0.37	RET: 0.025	1 mm	20 mm round	No

OPC ordinary Portland cement, *FA* coal fly ash, *GGBFS* ground granulated blast furnace slag, *RS* river sand, *W* water, *SH* sodium hydroxide, *SP* superplasticizer, *RET* retarder

(a)

(b)

(c)

Fig. 4 **a** A picture of Lutum V4 used for printing and comparison purposes in this study and **b**, **c** the auger and the extrusion system

standard industry ASTM mechanical testing. In addition, the use of dies additively manufactured using readily available polylactic acid thermoplastic allows users to manipulate die form without the use of machining or tooling, as similar to Ref. [49].

4.5.3 Auger screw extrusion

Screw-based extrusion is a heavily used technique for the extrusion of high viscosity materials, such as polymers, composites, and cements. The advantages of the screw-based extrusion system are multifold. The extrusion screw can be refilled continuously, the rotary motion of the screw can provide aggregate dispersion, and extrusion and retraction are possible, as in Fig. 6a, b. Based on this experiment, the use of a continuous extrusion system has been a major success whereby cement mortar has been successfully additively manufactured without any constraints on aggregate size [50].

5 Results

5.1 Printability

5.1.1 Lutum V4

A combination of materials rheology, correct particle size, and machine parameters affected the ability of the Lutum V4 printer to produce useable samples. In efforts to increase the capability of the Lutum V4 printer, a series of larger nozzles have been additively manufactured (using fused deposition method—also FDM) that can be seen in Fig. 7.

Table 6 presents the result of 18 mixes that have been used on Lutum V4 with various aggregates and nozzle sizes with their respective printability. As can be seen in this table, the majority of the attempts have been unsuccessful, regardless of the materials combination or nozzle sizes. This is due to not achieving the allowable viscosity of the mixed materials to have a successful printing. Also, the nature of the 3D printing of cementitious materials allows only a short time frame for the materials to be printed since the hardening process tends to increase the viscosity of the materials gradually. Figure 8, presents successful prints conducted with Lutum V4. Figure 8a shows the printing of cement paste exhibiting low shape retention under the weight of multiple layers. Figure 8b shows 3D printing of cement mortar with a maximum aggregate size of 1 mm. As can be seen in this figure, better shape retention and a more homogenous printing is achieved. Figure 8c presents the result of mix No. 8 printed with a 10 mm nozzle and a max aggregate size of 2 mm.

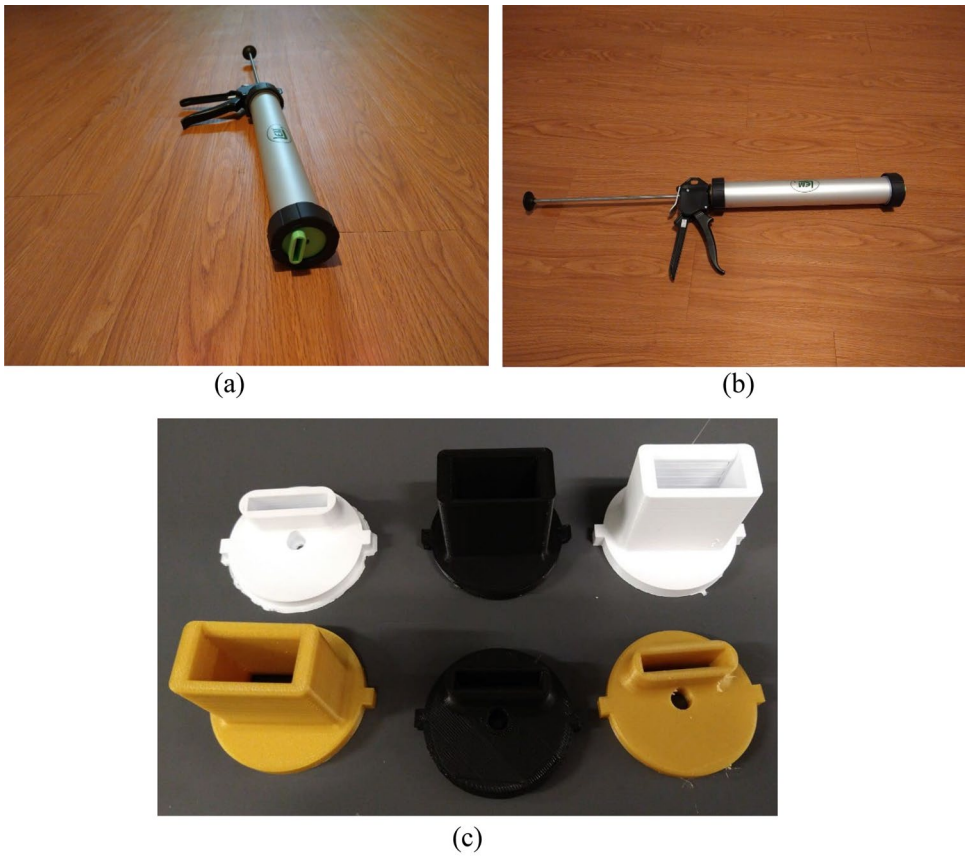

Fig. 5 **a**, **b** Mechanically actuated piston extruder and **c** various nozzle shapes printed for use in both piston and auger screw-based system

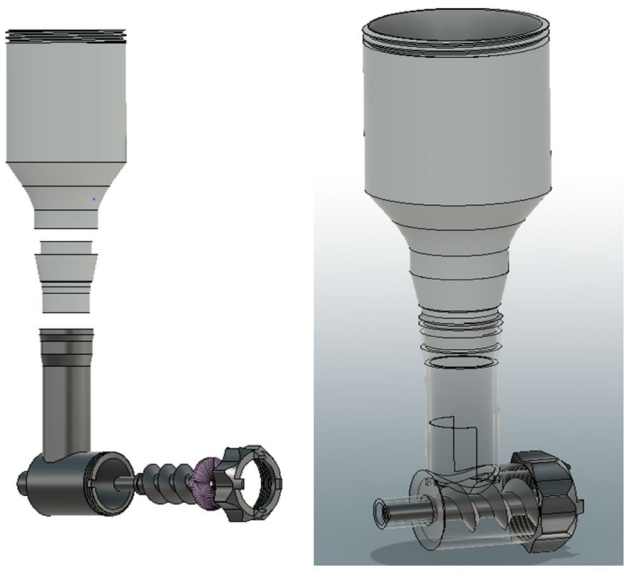

Fig. 6 Auger screw-based extrusion

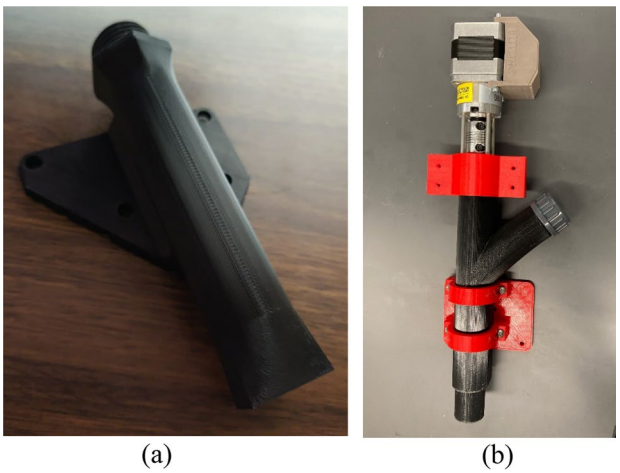

Fig. 7 **a**, **b** Different nozzle systems printed and used to enhance the printing of Lutum V4

5.1.2 Piston-based extrusion

The result of printability attempts conducted with the piston mechanism is documented in Table 7. As can be seen in this table, all of the mixes have been printed with relative ease, regardless of the nozzle size, aggregate size or mixture

(a)

(b)

(c)

Fig. 8 T3D-printed cementitious materials using Lutum V4.0, with **a** mix No. 3, **b** mix No. 6 and **c** mix No. 8

proportions. Using the nozzle size of 30 × 10 mm, as shown in Fig. 9, geopolymer mortar with sodium hydroxide activator has been successfully printed.

5.1.3 Auger screw extrusion

Table 8 presents the mixes that were printed with the auger-screw system. As can be seen, all of the mixes (from mix 27 through 32) have been successfully printed. Compared to the piston-based fixture, the samples printed with the screw-based fixture experienced a higher degree of inhomogeneity which can be due to human error, rather than the extrusion mechanism. In other words, since the instrument was guided by hand during the extrusion process, the resulting material exhibits inconsistency between layers. This can further be seen in Fig. 10.

5.2 Material properties

5.2.1 Flowability

To test the fresh property of the mortar, the flow table, a common testing instrument used in self-compacting concrete and mortar testing has been adopted, conforming to ASTM C1437 [51]. Based on the result of the flow table, and as can be seen in Fig. 11, the mixture had a spread diameter of 165 mm.

5.2.2 Compressive strength

To measure the compressive strength of printed materials, specimens with the size of 20 × 20 mm were sawn from larger printed samples. Specimen were then put in Automax compression testing machine according to ASTM C109 [53] under load control at the rate of 35 psi/s as in Ref. [20]. Figure 12 shows the position of the test and type of failure of each sample. Figure 13 shows the result of compressive strength test. Based on Fig. 13, screw-based specimen had a relatively higher compressive strength. This can be attributed to better material dispersion in presence of an auger that results in enhanced hydration of cementitious materials [54]. Another reason for this, according to Ref. [55], can be due to the speed of printing that can have significant influence on the porosity of the interlayer bonding region. In that respect, since the screw-based system used a smaller nozzle size, it would print layers at a faster rate than the piston based one. As noted by Ref. [56], as the time interval increases, the surface moisture of the layers is evaporated and when the next layer is deposited on top of the other, higher content of micro-pores are produced. This results in lower physico-mechanical properties [55, 56].

Table 7 Mixture ratios used to experiment with the piston extruder with values in ratio

Mix no.	FA	GGBFS	SH	Molarity	OPC	SP & RT (g)	W	R.S	Max Agg. size (mm)	Nozzle size (mm)	Printability
19	0.5	0.5	0.398	12	–	–	–	1	2	30×7	High slump
20	0.5	0.7	0.398	12	–	–	–	1	2	30×7	Yes
21	–	1	0.398	12	–	–	–	1	2	30×7	Yes
22	1	–	–	–	1	1.3	0.33	0.5	2	30×10	Yes
23	1	–	–	–	1	2.6	0.33	0.5	2	30×10	Yes
24	1	–	–	–	1	9.08	0.33	0.5	2	30×10	Yes
25	1	–	–	–	1	9.08	0.291.5	0.5	2	30×10	Yes
26	1	–	–	–	1	9.73	0.262	0.5	2	30×10	Yes

FA coal fly ash, *GGBFS* ground granulated blast furnace slag, *RS* river sand, *W* water, *SH* sodium hydroxide, *SP* superplasticizer, *RET* retarder

Fig. 9 Illustration of 3D-printed concrete with piston extruder

Table 8 Mixture proportions used for experimenting with the screw-based extrusion system

Mix No	OPC	FA	GGBFS	Water	SP & RT (g)	Aggregate	Max aggregate size (mm)	Nozzle size (mm)	Printability
27	1	0.5	0.5	0.33	1.3	0.5	2	30×7	Yes
28	1	0.5	0.5	0.33	2.6	0.5	2	30×7	Yes
29	1	1	–	0.33	2.6	0.5	2	30×7	Yes
30	1	1	–	0.291.5	9.08	0.5	2	30×7	Yes
31	1	1	–	0.262	9.08	0.5	2	30×7	Yes
32	1	1	–	0.25	9.73	0.5	2	30×7	Yes

OPC ordinary Portland cement, *FA* coal fly ash, *GGBFS* Ground granulated blast furnace slag, *RS* river sand, *W* water, *SH* sodium hydroxide, *SP* superplasticizer, *RET* retarder

Fig. 10 Printed mixes using auger screw system using mix No. 20

5.2.3 Flexural strength

For testing flexural strength of the specimen, 40 mm × 135 mm printed material specimens were sawn and put under a flexural testing machine with a load rating conforming to the loading rate of ASTM C348 [57]. Based on Fig. 14, the piston-based extruder samples had a relatively higher flexural strength which can be attributed to the lower number of layers, resulting in potentially reduced inter-layer porosity [58]. This can be due to faster printing time of piston-based system, which in this instance, since both modules were used manually, the speed of printing was

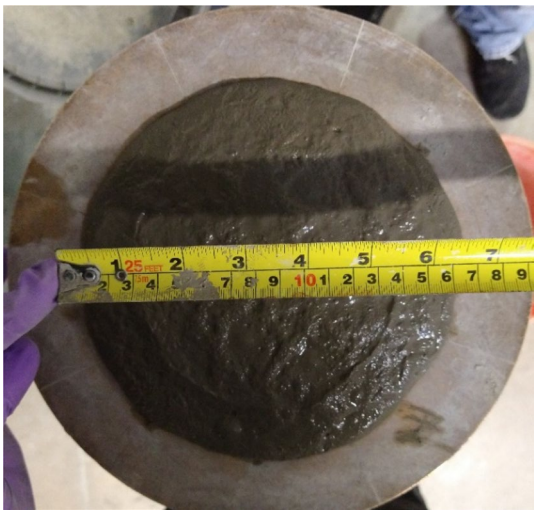

Fig. 11 Result of flow table test, conforming to ASTM C1437 [52]

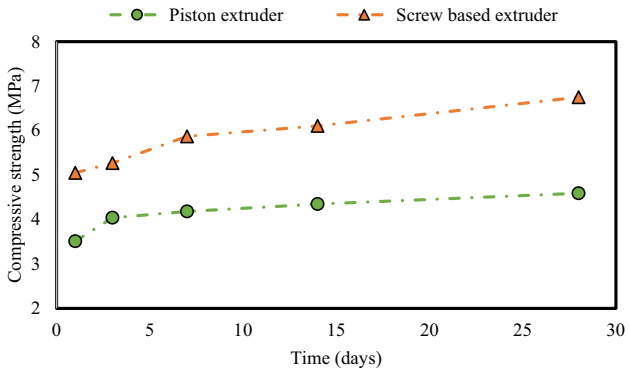

Fig. 13 Result of compressive strength test (ASTM C109) conducted on the printed specimen by screw-based system compared to piston-based extruder

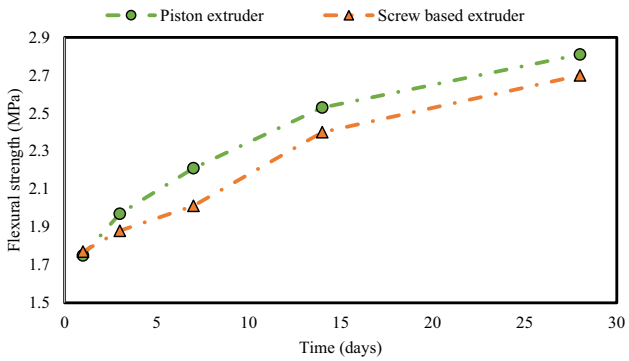

Fig. 14 Result of the flexural strength test (ASTM C348) conducted on the printed specimen by the screw-based system compared to a piston-based extruder

not measured. However, as discussed in Refs. [23, 59] that the speed of printing can have significant impact on the overall strength and even pore distribution. Figure 15 shows the failure type of the tested specimens.

5.2.4 Sample quality

Although the piston-based extrusion mechanism provided a low-cost mechanism for concrete extrusion, it was noted that the dispersion of the resulting extrusions was poor. This is likely due to the settling of aggregates out of the mortar due to the absence of any mixing action or vibration [60]. In addition, the piston-based extrusion is constrained by its container size. The mechanism is only capable of extruding its reservoirs volume at a time before requiring disassembly for material replenishment. This discontinuous system is capable of providing small samples for material characterization but would not be suitable for additive manufacturing of concretes.

Due to the higher layer height of the piston extrusion samples, larger drying shrinkage values were observed in comparison to screw extruder samples. Additionally, samples experienced a relatively large number of micro-pores and air-void pores, possibly due to lack of vibration [60] as

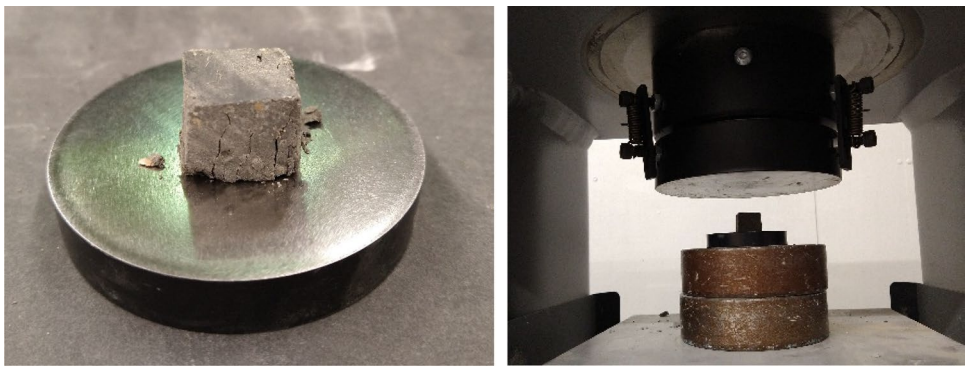

Fig. 12 **a** Showing the type of failure of cube specimen and **b** its respective position prior to the compression test

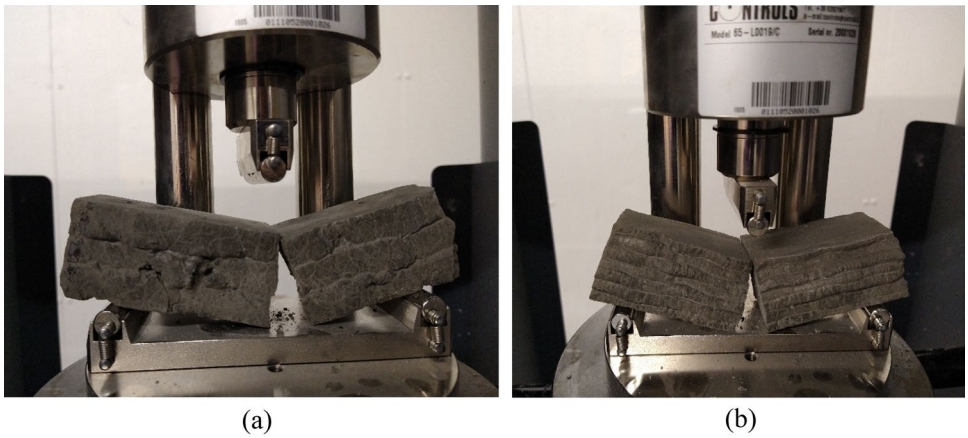

Fig. 15 Failure under flexural strength test for specimen printed by piston-based extruder (**a**) and auger screw-based extruder system (**b**)

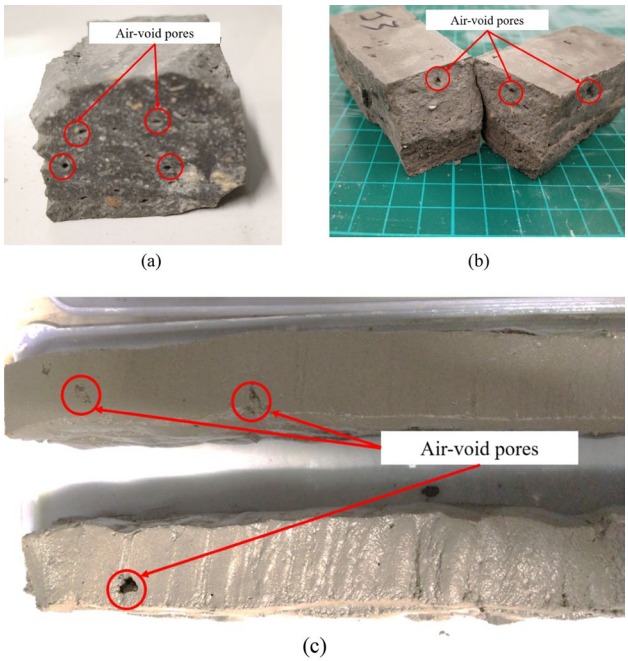

Fig. 16 Void formation within extruded samples with (**a**) and **c** piston printed, **b** screw-based printed

compared to conventionally cast concrete. This is further presented in Fig. 16.

5.2.5 Drying shrinkage

To evaluate the shrinkage tendency of the produced samples, they were cut to with the size of 40 mm × 135 mm sizes and put in a curing chamber to imitate the conditions advised by ASTM C596 [61]. Figure 17a, b shows the samples cut to size for this test and Fig. 17c presents the results of drying shrinkage values. Based on this figure, at the 28th day of curing, the specimens extruded by piston have a micro strain value of ~ 163 while those printed with screw-based fixture have a value of ~ 144 micro strain. This

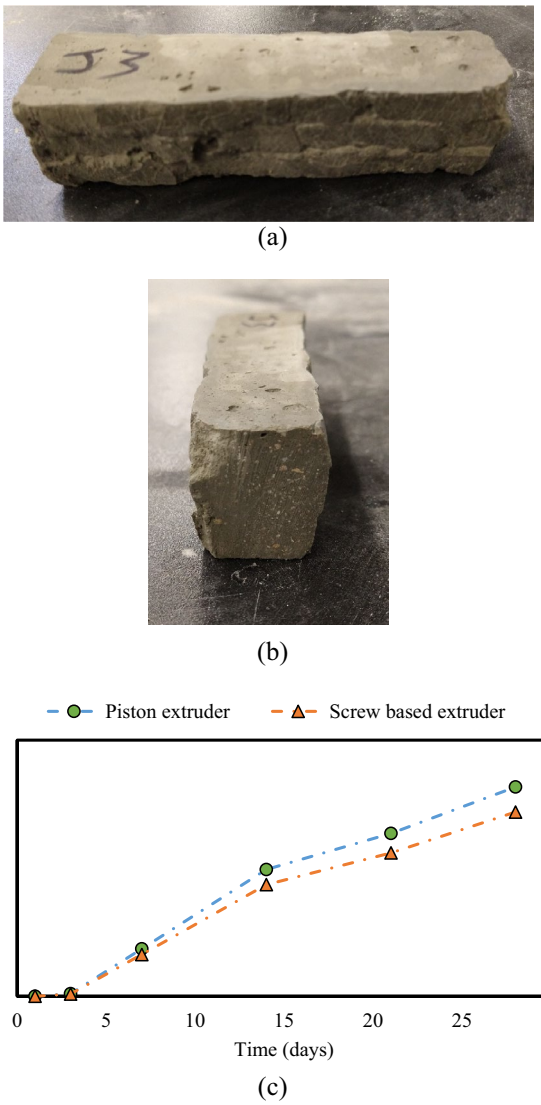

Fig. 17 Drying shrinkage of piston and screw based printed materials

shows that a slightly higher drying shrinkage values are achieved when piston-based fixture is used. This can be due to the presence of higher air-cavities on the surface of the piston printed sections that lowers the ability of the printed materials to withstand the contracting force of shrinkage [62, 63]. As noted by Ref. [64], the lower content of internal solid materials result in the increased effect of shrinkage and higher micro strain values.

6 Conclusions and discussion

In general, to 3D print cementitious materials, there are a few challenges that should first be addressed that include the material setting time of the mixture, viscosity of the freshly mixed materials, and aggregate sizes. Successful results of printed samples and the mechanical property tests support the use of the introduced modular lightweight additive manufacturing system for 3D printing cementitious materials based on screw-based extrusion using simple to create thermoplastic dies. The system provides a simple designed extruder for mounting onto gantry or robotic arms for automated printing. As in any other additive manufacturing technique, an automated process is expected to take place which, in most 3D printing cementitious materials is conducted through a control arm. In our auger screw extrusion system, although it has been used in absence of an automated arm, it clearly shows potential for a constant feeding system connected to an automated control arm. In general, the results of this study may be summarized as the following:

- The effect of nozzle size is found to be of lower significance in the piston-based system due to the simplicity and lack of auger in that system. However, based on previous studies and the findings of this research, the ratio of nozzle diameter to the aggregate size of 1:5 is an ideal approach to prevent nozzle obstruction during extrusion.
- In 3D printing, materials dispersion is a critical factor that can affect the final physico-mechanical properties of the printed samples. The screw-based systems ability to provide material mixing through its rotating screw, produced better compressive strength results. Nonetheless, since in this study, both piston and screw-based modules were used manually, the speed of printing was higher for piston-based system which resulted in better flexural strength.
- The result of drying shrinkage test further supported the significance of materials dispersion and printing time interval of each layer that can significantly affect the porosity of the printed sections which can have direct effect on the shrinkage tendency of the printed materials.

The result of this study point to the potential use of the piston or screw-based systems as an affordable alternative to commercially available 3D printers for cementitious materials. Further experimentation is required to hone the linear advance, extrusion rates, and slicing associated with the automated printing using this low-cost alternative.

Acknowledgements The author cordially appreciates the use of the Texas State University Ingram Hall Makerspace in providing both expertise and machinery for producing our prototypes. In addition, we appreciate Texas State University providing the ground for our educational exploration with the freedom to develop new and interesting ideas.

Data availability The authors also declare that no data has been used during or for the purpose of this research study.

Declarations

Conflict of interest The authors declare that they have no known competing financial interests or personal relationships that could have appeared to influence the work reported in this paper.

References

1. Nodehi M, Ozbakkaloglu T, Gholampour A (2022) Effect of supplementary cementitious materials on properties of 3D printed conventional and alkali-activated concrete: a review. Autom Constr 138:104215. https://doi.org/10.1016/j.autcon.2022.104215
2. Nodehi M, Aguayo F, Nodehi SE, Gholampour A, Ozbakkaloglu T, Gencel O (2022) Durability properties of 3D printed concrete (3DPC). Autom Constr 142:104479. https://doi.org/10.1016/j.autcon.2022.104479
3. Terry S et al (2020) The influence of smart manufacturing towards energy conservation: a review. Technologies 8(2):31. https://doi.org/10.3390/technologies8020031
4. Shakeri Z, Benfriha K (2022) An overview on smart scheduling in MES: in the context of industry 4.0. In: *2022 27th International Conference on Automation and Computing (ICAC)*, Bristol, United Kingdom, 2022, pp 1–6. doi: https://doi.org/10.1109/ICAC55051.2022.9911166.
5. Bruzzone L, Molfino RM (2006) A novel parallel robot for current microassembly applications. Assem Autom 26(4):299–306. https://doi.org/10.1108/01445150610705218
6. Fanghella P, Bruzzone L, Ellero S, Landò R (2016) Kinematics, efficiency and dynamic balancing of a planetary gear train based on nutating bevel gears. Mech Based Des Struct Mach 44(1–2):72–85. https://doi.org/10.1080/15397734.2015.1047956
7. Bruzzone L, Bozzini G (2011) A statically balanced SCARA-like industrial manipulator with high energetic efficiency. Meccanica 46(4):771–784. https://doi.org/10.1007/s11012-010-9336-6
8. kumar AV (2022) A review paper on 3D-printing and various processes used in the 3D-printing. IJSREM. https://doi.org/10.55041/IJSREM13278
9. Khoshnevis B (2004) Automated construction by contour crafting-related robotics and information technologies. Autom Constr 13(1):5–19. https://doi.org/10.1016/j.autcon.2003.08.012
10. Zhang J, Wang J, Dong S, Yu X, Han B (2019) A review of the current progress and application of 3D printed concrete. Compos Part A Appl Sci Manuf 125(1):105533. https://doi.org/10.1016/j.compositesa.2019.105533

11. Mechtcherine V et al (2021) Integrating reinforcement in digital fabrication with concrete: A review and classification framework. Cem Concr Compos 119:103964. https://doi.org/10.1016/j.cemconcomp.2021.103964
12. Sanjayan JG, Nematollahi B, Xia M, Marchment T (2018) Effect of surface moisture on inter-layer strength of 3D printed concrete. Constr Build Mater 172:468–475. https://doi.org/10.1016/j.conbuildmat.2018.03.232
13. Shakeri Z, Benfriha K, Zirak N, Shirinbayan M (2022) Mechanical strength and shape accuracy optimization of polyamide FFF parts using grey relational analysis. Sci Rep 12(1):13142. https://doi.org/10.1038/s41598-022-17302-z
14. Buswell RA, Leal de Silva WR, Jones SZ, Dirrenberger J (2018) 3D printing using concrete extrusion: a roadmap for research. Cem Concr Res 112(June):37–49. https://doi.org/10.1016/j.cemconres.2018.05.006
15. Zhang C, Hou Z, Chen C, Zhang Y, Mechtcherine V, Sun Z (2019) Design of 3D printable concrete based on the relationship between flowability of cement paste and optimum aggregate content. Cem Concr Compos 104(September):103406. https://doi.org/10.1016/j.cemconcomp.2019.103406
16. Moelich GM, Kruger J, Combrinck R (2020) Plastic shrinkage cracking in 3D printed concrete. Compos Part B Eng 200(July):108313. https://doi.org/10.1016/j.compositesb.2020.108313
17. Ding T, Xiao J, Zou S, Wang Y (2020) Hardened properties of layered 3D printed concrete with recycled sand. Cem Concr Compos 113(June):103724. https://doi.org/10.1016/j.cemconcomp.2020.103724
18. Panda B, Mohamed NAN, Paul SC, Singh GVPB, Tan MJ, Šavija B (2019) The effect of material fresh properties and process parameters on buildability and interlayer adhesion of 3D printed concrete. Materials. https://doi.org/10.3390/ma12132149
19. Lim JH, Panda B, Pham QC (2018) Improving flexural characteristics of 3D printed geopolymer composites with in-process steel cable reinforcement. Constr Build Mater 178:32–41. https://doi.org/10.1016/j.conbuildmat.2018.05.010
20. Zhang Y, Zhang Y, She W, Yang L, Liu G, Yang Y (2019) Rheological and harden properties of the high-thixotropy 3D printing concrete. Constr Build Mater 201:278–285. https://doi.org/10.1016/j.conbuildmat.2018.12.061
21. Chen Y et al (2020) Effect of printing parameters on interlayer bond strength of 3D printed limestone-calcined clay-based cementitious materials: an experimental and numerical study. Constr Build Mater. https://doi.org/10.1016/j.conbuildmat.2020.120094
22. Wolfs RJM, Bos FP, Salet TAM (2019) Hardened properties of 3D printed concrete: The influence of process parameters on interlayer adhesion. Cem Concr Res 119(January):132–140. https://doi.org/10.1016/j.cemconres.2019.02.017
23. Tay YWD, Ting GHA, Qian Y, Panda B, He L, Tan MJ (2019) Time gap effect on bond strength of 3D-printed concrete. Virtual and Physical Prototyping 14(1):104–113. https://doi.org/10.1080/17452759.2018.1500420
24. Federowicz K, Kaszyńska M, Zieliński A, Hoffmann M (2020) Effect of curing methods on shrinkage development in 3D-printed concrete. Materials. https://doi.org/10.3390/ma13112590
25. Ding T, Xiao J, Zou S, Zhou X (2020) Anisotropic behavior in bending of 3D printed concrete reinforced with fibers. Compos Struct 254(July):112808. https://doi.org/10.1016/j.compstruct.2020.112808
26. Wang L, Jiang H, Li Z, Ma G (2020) Mechanical behaviors of 3D printed lightweight concrete structure with hollow section. Arch Civ Mech Eng 20(1):1–17. https://doi.org/10.1007/s43452-020-00017-1
27. Ju Y et al (2017) Visualization of the three-dimensional structure and stress field of aggregated concrete materials through 3D printing and frozen-stress techniques. Constr Build Mater 143:121–137. https://doi.org/10.1016/j.conbuildmat.2017.03.102
28. Le TT et al (2012) Hardened properties of high-performance printing concrete. Cem Concr Res 42(3):558–566. https://doi.org/10.1016/j.cemconres.2011.12.003
29. Pham L, Tran P, Sanjayan J (2020) Steel fibres reinforced 3D printed concrete: Influence of fibre sizes on mechanical performance. Constr Build Mater 250:118785. https://doi.org/10.1016/j.conbuildmat.2020.118785
30. Panda B, Paul SC, Mohamed NAN, Tay YWD, Tan MJ (2018) Measurement of tensile bond strength of 3D printed geopolymer mortar. Measurement 113(September 2017):108–116. https://doi.org/10.1016/j.measurement.2017.08.051
31. Cicione A, Kruger J, Walls RS, Van Zijl G (2021) An experimental study of the behavior of 3D printed concrete at elevated temperatures. Fire Saf J 120(January):103075. https://doi.org/10.1016/j.firesaf.2020.103075
32. Joh C, Lee J, Bui TQ, Park J, Yang IH (2020) Buildability and mechanical properties of 3d printed concrete. Materials 13(21):1–24. https://doi.org/10.3390/ma13214919
33. Ting GHA, Tay YWD, Qian Y, Tan MJ (2019) Utilization of recycled glass for 3D concrete printing: rheological and mechanical properties. J Mater Cycles Waste Manag 21(4):994–1003. https://doi.org/10.1007/s10163-019-00857-x
34. Lim JH, Zhang X, Ting GHA, Pham QC (2021) Stress-cognizant 3D printing of free-form concrete structures. J Build Eng 39(October 2020):102221. https://doi.org/10.1016/j.jobe.2021.102221
35. Ye J, Cui C, Yu J, Yu K, Xiao J (2021) Fresh and anisotropic-mechanical properties of 3D printable ultra-high ductile concrete with crumb rubber. Compos Part B Eng 211(November 200):108639. https://doi.org/10.1016/j.compositesb.2021.108639
36. vormvrij.nl/, "The Lutum
37. A. International (2001) ASTM C136–01, Standard Test Method for Sieve Analysis of Fine and Coarse Aggregates. ASTM International, West Conshohocken, PA, i(200): 1–5. https://doi.org/10.1520/C0136-01.
38. ASTM C128–15 (2015) Standard Test Method for Relative Density (Specific Gravity) and Absorption of Coarse Aggregate. Annu Book ASTM Stand i:1–5. https://doi.org/10.1520/C0128-15.2
39. Valkenaers H, Vogeler F, Voet A, Kruth JP Screw extrusion based 3D printing, a novel additive manufacturing technology, p. 7
40. Xu W et al (2021) 3D printing for polymer/particle-based processing: a review. Compos Part B Eng 223:109102. https://doi.org/10.1016/j.compositesb.2021.109102
41. Joshi SC, Sheikh AA (2015) 3D printing in aerospace and its long-term sustainability. Virtual Phys Prototyping 10(4):175–185. https://doi.org/10.1080/17452759.2015.1111519
42. Gosselin C, Duballet R, Roux P, Gaudillière N, Dirrenberger J, Morel P (2016) Large-scale 3D printing of ultra-high performance concrete—a new processing route for architects and builders. Mater Des 100:102–109. https://doi.org/10.1016/j.matdes.2016.03.097
43. Ma G, Salman NM, Wang L, Wang F (2020) A novel additive mortar leveraging internal curing for enhancing interlayer bonding of cementitious composite for 3D printing. Constr Build Mater 244:118305. https://doi.org/10.1016/j.conbuildmat.2020.118305
44. ASTM C 109, C 109M–02 (2005) Standard test method for compressive strength of hydraulic cement mortars. Annu Book ASTM Stand 04:9. https://doi.org/10.1520/C0109
45. Rahul AV, Santhanam M, Meena H, Ghani Z (2019) Mechanical characterization of 3D printable concrete. Constr Build Mater 227:116710. https://doi.org/10.1016/j.conbuildmat.2019.116710
46. Heras Murcia D, Genedy M, Reda Taha MM (2020) Examining the significance of infill printing pattern on the anisotropy of 3D printed concrete. Constr Build Mater 262:120559. https://doi.org/10.1016/j.conbuildmat.2020.120559

47. ASTM C39, C39M (2003) Standard test method for compressive strength of cylindrical concrete specimens 1. ASTM Stand Book i:1–5. https://doi.org/10.1520/C0039
48. Alchaar AS, Al-Tamimi AK (2021) Mechanical properties of 3D printed concrete in hot temperatures. Constr Build Mater 266:120991. https://doi.org/10.1016/j.conbuildmat.2020.120991
49. Kim NP, Eo J-S, Cho D (2018) Optimization of piston type extrusion (PTE) techniques for 3D printed food. J Food Eng 235:41–49. https://doi.org/10.1016/j.jfoodeng.2018.04.019
50. Gomaa M, Jabi W, Veliz Reyes A, Soebarto V (2021) 3D printing system for earth-based construction: Case study of cob. Autom Constr 124:103577. https://doi.org/10.1016/j.autcon.2021.103577
51. ASTM, C143M-15a (2009) Standard test method for slump of hydraulic cement concrete (C 143). ASTM Int 27:99–101. https://doi.org/10.1520/C1437-15.2
52. Astm (2001) Standard test method for flow of hydraulic cement mortar: C1437–01. Standard, pp 7–8, doi: https://doi.org/10.1520/C1437-15.2.
53. A. C109, 109M-16a (2016) Standard test method for compressive strength of hydraulic cement mortars (Using 2-in. or cube specimens). Annu Book ASTM Stand i:1–10. https://doi.org/10.1520/C0109
54. Perrot A, Rangeard D, Courteille E (2018) 3D printing of earth-based materials: processing aspects. Constr Build Mater 172:670–676. https://doi.org/10.1016/j.conbuildmat.2018.04.017
55. Nerella VN, Hempel S, Mechtcherine V (2019) Effects of layer-interface properties on mechanical performance of concrete elements produced by extrusion-based 3D-printing. Constr Build Mater 205:586–601. https://doi.org/10.1016/j.conbuildmat.2019.01.235
56. Marchment T, Sanjayan J, Xia M (2019) Method of enhancing interlayer bond strength in construction scale 3D printing with mortar by effective bond area amplification. Mater Des 169:107684. https://doi.org/10.1016/j.matdes.2019.107684
57. ASTM C348 (1998) Standard test method for flexural strength of hydraulic-cement mortars. Annu Book ASTM Stand 04:2–7. https://doi.org/10.1520/C0348-14.2
58. Van Der Putten J, Deprez M, Cnudde V, De Schutter G, Van Tittelboom K (2019) Microstructural characterization of 3D printed cementitious materials. Materials. https://doi.org/10.3390/ma12182993
59. Babafemi AJ, Kolawole JT, Miah MJ, Paul SC, Panda B (2021) A concise review on interlayer bond strength in 3D concrete printing. Sustainability 13(13):7137. https://doi.org/10.3390/su13137137
60. Yu S, Xia M, Sanjayan J, Yang L, Xiao J, Du H (2021) Microstructural characterization of 3D printed concrete. J Build Eng 44(February):102948. https://doi.org/10.1016/j.jobe.2021.102948
61. ASTM Committee C01.31 (2007) ASTM C596–07 Standard test method for drying shrinkage of mortar containing hydraulic cement. Annu Book oASTM Stand Vol 04.01 11(5):1–3. https://doi.org/10.1520/C0596-09
62. Sivarupan T et al (2021) A review on the progress and challenges of binder jet 3D printing of sand moulds for advanced casting. Addit Manuf 40:101889. https://doi.org/10.1016/j.addma.2021.101889
63. Slowik V, Schmidt M, Fritzsch R (2008) Capillary pressure in fresh cement-based materials and identification of the air entry value. Cem Concr Compos 30(7):557–565. https://doi.org/10.1016/j.cemconcomp.2008.03.002
64. Gencel O et al (2022) Lightweight foam concrete containing expanded perlite and glass sand: Physico-mechanical, durability, and insulation properties. Constr Build Mater 320(January):126187. https://doi.org/10.1016/j.conbuildmat.2021.126187